

Stochastic Filtering Using Periodic Cost Functions

EYAL NITZAN
TIRZA ROUTTENBERG
JOSEPH TABRIKIAN

Stochastic filters attempt to estimate an unobservable state of a stochastic dynamical system from a set of noisy measurements. In this paper, we consider circular stochastic filtering and develop two dynamic methods for estimation of circular states, named sample-based stochastic filtering via root-finding (SB-SFRF) and Fourier-based stochastic filtering via root-finding (FB-SFRF). The proposed SB-SFRF and FB-SFRF methods attempt to dynamically minimize Bayes periodic risks by using Fourier series representation of their corresponding cost functions. The performance of the proposed methods is evaluated in the problem of direction-of-arrival (DOA) tracking.

Manuscript received November 7, 2015; revised March 4, 2016; released for publication May 18, 2016. Refereeing of this contribution was handled by Dr. Gerhard Kurz.

Autors' address: Department of Electrical and Computer Engineering, Ben-Gurion University of the Negev, Beer-Sheva 84105, Israel (E-mail: eyalni@ee.bgu.ac.il, tirzar@bgu.ac.il, joseph@bgu.ac.il).

This research was partially supported by THE ISRAEL SCIENCE FOUNDATION (grant No. 1160/15).

1557-6418/16/\$17.00 © 2016 JAIF

1. INTRODUCTION

In stochastic filtering problems, it is required to estimate the state of a dynamic system using a sequence of noisy measurements. Bayesian stochastic filtering is a commonly-used estimation technique that based on a state space model, recursively updates the posterior probability density function (pdf) of the current state given current and previous measurements. Under a chosen risk, optimal estimators can be obtained from the posterior pdf at each time step.

The mean-squared-error (MSE) risk is widely used for performance evaluation in stochastic filtering problems. Due to the dynamic nature of these problems, computation/approximation of the minimum MSE (MMSE) estimator is performed recursively by using stochastic filters and recursive computation of the posterior pdf. For linear dynamic systems with Gaussian noise, the well-known Kalman filter [17] provides, at each time step, a closed-form expression for the MMSE estimator. However, for the general nonlinear and/or non-Gaussian case there is no optimal filtering method that provides an analytic expression for the MMSE estimator or for the MMSE performance. Suboptimal filtering methods include the extended Kalman filter (e.g. [1], [12], [16], [56]), the unscented Kalman filter (e.g. [15], [51]), as well as discrete (approximate grid-based) filters and particle filters (e.g. [2], [10], [13]).

In many stochastic filtering problems, the unknown state has a circular nature, for example, phase, frequency, and direction-of-arrival (DOA) (see e.g. [26], [43], [55], [59]). We denote these problems as circular stochastic filtering problems. In this case, at each time step, we are interested in the modulo- 2π estimation errors and not in the plain error values. In fact, the plain error values may be absurd for estimation of circular states, especially if the unknown state is close to the edges of the circular domain [31], [45], [49]. Thus, the MSE risk and the MMSE estimator are inappropriate for circular stochastic filtering and alternative periodic risks that are based on 2π -periodic cost functions, should be used [5], [37], [38], [40], [49]. As a result, recursively-computed estimators under these periodic risks should be derived.

Several circular estimation methods, also known as directional estimation methods, have been proposed for obtaining estimators under periodic risks in static estimation problems. In [57] and [58], infinite-dimensional equations for optimal estimation under periodic risks are derived by using infinite Fourier series. However, the solution to these infinite-dimensional equations is not presented. In [47], the parameter estimation via root-finding (PERF) method is proposed. The PERF method expresses 2π -periodic cost functions via their Fourier series and derives corresponding optimal Bayes estimators for these cost functions, by using a polynomial root-finding algorithm. This method is computationally

manageable and avoids a grid search for the optimal estimator. A new approach for estimating the mean direction of a circular random variable is presented in [35], based on the minimum squared arc length criterion.

There are two main approaches in the literature for circular stochastic filtering that utilize the circular nature of the state. In [3], [20]–[23], [33], circular filters attempt to estimate the current posterior pdf under the assumption that it belongs to specific distributions on the circle. The second approach is representing the posterior pdf via a Fourier series, without assuming any specific distribution, and predicting/updating its Fourier coefficients. In [7], this approach was utilized for nonlinear filtering on linear domains under a general state and measurement model. Circular filters that utilize this approach are proposed in [57], [58] for a specific state model and in [44] for a more general state model. The circular filter in [44] maintains a valid approximation for the posterior pdf by efficiently predicting and updating the Fourier coefficients of its square root and normalizing it accordingly.

In general stochastic filtering problems and in particular in circular problems, the posterior pdf, from which the state is estimated, is usually computed or approximated. In circular stochastic filtering problems, the circular mean of the posterior pdf, which describes the pdf location on the circle, is usually used as an estimator of the circular state (see e.g. [20], [21], [44], [53]). However, the posterior circular mean is not the optimal estimator under a general periodic risk [47].

In this paper, we consider discrete-time circular stochastic filtering problems. We propose two methods for circular stochastic filtering via root-finding (SFRF): the sample-based SFRF (SB-SFRF) and the Fourier-based SFRF (FB-SFRF). The proposed methods enable the implementation of PERF method from [47], which is suitable for off-line estimation with batch data, for filtering problems, where the data is processed sequentially. The SB-SFRF and FB-SFRF methods derive estimators under a general periodic Bayes risk in circular stochastic filtering problems. The two methods are based on representation of the corresponding periodic cost function by a Fourier series and then, implementation of a root-finding algorithm. The SB-SFRF method approximates the current posterior pdf with a finite sum of weighted Dirac components while the FB-SFRF method approximates the posterior pdf with a finite Fourier series. We examine the following periodic cost functions: 1) squared-periodic-error (SPE) (see e.g. [22], [48]); 2) absolute-periodic-error (APE) (see e.g. [32, pp. 19–20], [36]); and 3) cyclic-error (CE) (see e.g. [3], [39], [50], [57]). The performance of the proposed SB-SFRF and FB-SFRF methods is demonstrated in the problem of DOA tracking.

The remainder of the paper is organized as follows. In Section 2, we formulate the circular stochastic filtering model and review the properties of common periodic risks. In Section 3, the SB-SFRF and FB-SFRF

methods are derived. The proposed methods are evaluated via simulations for DOA tracking problem in Section 4. Finally, our conclusions appear in Section 5.

In the sequel, we denote vectors and matrices by boldface lowercase and uppercase letters, respectively. The m th element of the vector \mathbf{b} is denoted by b_m and $j \triangleq \sqrt{-1}$. The notations $(\cdot)^T$ and $(\cdot)^*$ denote the transpose and complex conjugate operators, respectively. The notation $\angle \cdot$ stands for the phase of a complex scalar, which is assumed to be restricted to the interval $[-\pi, \pi)$. The modulo- 2π operator, which maps $\rho \in \mathbb{R}$ to $[-\pi, \pi)$, is denoted as $[\rho]_{2\pi} \triangleq \rho - 2\pi \lfloor \frac{\rho}{2\pi} + \frac{1}{2} \rfloor$, where $\lfloor \cdot \rfloor$ is the floor operator. The operators of expectation and conditional expectation given an event Z , are denoted as $E[\cdot]$ and $E[\cdot | Z]$, respectively.

2. CIRCULAR STOCHASTIC FILTERING

Consider the following nonlinear discrete-time state space model

$$\begin{cases} \theta_n = a_n(\theta_{n-1}, \mathbf{w}_n) \\ \mathbf{x}_n = \mathbf{h}_n(\theta_n, \boldsymbol{\nu}_n) \end{cases}, \quad n = 1, 2, \dots, \quad (1)$$

where for any $n = 1, 2, \dots$

- $\theta_n \in \Omega_\theta \triangleq [-\pi, \pi)$ —circular state for which we are interested in the modulo- 2π estimation error.
- $\theta_0 \in \Omega_\theta$ —initial state with known a priori pdf f_{θ_0} .
- $\mathbf{x}_n \in \mathbb{C}^L$ —measurement vector.
- $\{\mathbf{w}_n\}$ —sequence of mutually independent $P \times 1$ noise vectors with known pdfs, $\{f_{\mathbf{w}_n}\}$, that are independent of past and present states.
- $\{\boldsymbol{\nu}_n\}$ —sequence of mutually independent $Q \times 1$ complex noise vectors with known pdfs, $\{f_{\boldsymbol{\nu}_n}\}$, that are independent of past and present states and the state noise.
- $a_n : \Omega_\theta \times \mathbb{R}^P \rightarrow \Omega_\theta$ —state transition function.
- $\mathbf{h}_n : \Omega_\theta \times \mathbb{C}^Q \rightarrow \mathbb{C}^L$ —measurement function.

The conditional pdfs $f_{\theta_n|\theta_{n-1}}$ and $f_{\mathbf{x}_n|\theta_n}$ can be obtained from (1) and the pdfs of \mathbf{w}_n and $\boldsymbol{\nu}_n$, respectively. The filtering goal is to estimate the circular state θ_n at each time step $n = 1, 2, \dots$, based on $\mathbf{x}^{(n)} \triangleq [\mathbf{x}_1^T, \dots, \mathbf{x}_n^T]^T \in \Omega_{\mathbf{x}}^{(n)}$, which is the augmented measurement vector containing all the measurements up to time step n , where $\Omega_{\mathbf{x}}^{(n)}$ is the n th step measurement space. An estimator of θ_n , based on $\mathbf{x}^{(n)}$, is denoted by $\hat{\theta}_n : \Omega_{\mathbf{x}}^{(n)} \rightarrow \Omega_\theta$. The posterior pdf of θ_n given $\mathbf{x}^{(n)}$ and the predicted pdf of θ_n given $\mathbf{x}^{(n-1)}$ are denoted by $f_{\theta_n|\mathbf{x}^{(n)}}$ and $f_{\theta_n|\mathbf{x}^{(n-1)}}$, respectively, $\forall n = 1, 2, \dots$, where $f_{\theta_1|\mathbf{x}^{(0)}} \triangleq f_{\theta_1}$ denotes the a priori pdf of $\theta_1 \in \Omega_\theta$. In addition, we define $f_{\theta_0|\mathbf{x}^{(0)}} \triangleq f_{\theta_0}$.

In the Bayesian framework, optimal estimators are obtained via minimization of Bayes risks. In circular stochastic filtering problems, the appropriate Bayes risk at time step n is based on 2π -periodic cost function,

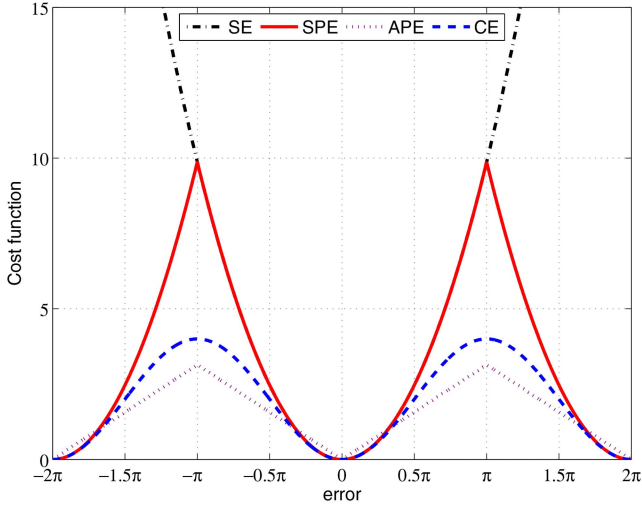


Fig. 1. SE and periodic cost functions: SPE, APE, and CE.

$C(\hat{\theta}_n - \theta_n)$, with respect to (w.r.t.) the estimation error, $\hat{\theta}_n - \theta_n$. The corresponding risk is the mean of the cost function, $E[C(\hat{\theta}_n - \theta_n)]$. It should be noted that restriction of the state estimator to the region $[-\pi, \pi]$ does not prevent the resulting estimation error from taking values in the region $(-2\pi, 2\pi)$. Thus, the inappropriate nature of the conventional risks, such as the MSE, cannot be resolved. For example, consider the case of close parameter and its estimate on the circle, in which $\theta_n = -\pi + \delta_1$ and $\hat{\theta}_n = \pi - \delta_2$, $0 < \delta_i \ll 1$, $i = 1, 2$. In this case, direct computation of the error results in $\hat{\theta}_n - \theta_n = 2\pi - (\delta_1 + \delta_2)$, which is a large error. However, computation of the periodic error results in $[\hat{\theta}_n - \theta_n]_{2\pi} = -(\delta_1 + \delta_2)$, which is a small error.

In the following, we describe three examples for periodic cost functions: SPE, APE, and CE. These periodic cost functions and the nonperiodic squared-error (SE) cost function are presented in Fig. 1 versus the estimation error. It can be seen that as the absolute value of the estimation error grows from π to 2π , the SE cost function increases, since it does not take the circular nature of the error into account, while the periodic cost functions decrease.

- SPE: The SPE cost function at the n th time step is defined as

$$C(\hat{\theta}_n - \theta_n) = \text{SPE}(\hat{\theta}_n - \theta_n) \triangleq ([\hat{\theta}_n - \theta_n]_{2\pi})^2. \quad (2)$$

Given a measurement vector, $\mathbf{x}^{(n)}$, the minimum mean SPE (MMSPE) estimator is given by

$$\hat{\theta}_{n,\text{MMSPE}} = \arg \min_{\hat{\theta}_n \in \Omega_\theta} E[(\hat{\theta}_n - \theta_n)_{2\pi}^2 | \mathbf{x}^{(n)}]. \quad (3)$$

- APE: The APE cost function at the n th time step is defined as

$$C(\hat{\theta}_n - \theta_n) = \text{APE}(\hat{\theta}_n - \theta_n) \triangleq |[\hat{\theta}_n - \theta_n]_{2\pi}|. \quad (4)$$

Given a measurement vector, $\mathbf{x}^{(n)}$, the minimum mean APE (MMAPE) estimator is given by

$$\hat{\theta}_{n,\text{MMAPE}} = \arg \min_{\hat{\theta}_n \in \Omega_\theta} E[|[\hat{\theta}_n - \theta_n]_{2\pi}| | \mathbf{x}^{(n)}]. \quad (5)$$

- CE: The CE cost function at the n th time step is defined as

$$C(\hat{\theta}_n - \theta_n) = \text{CE}(\hat{\theta}_n - \theta_n) \triangleq 2 - 2 \cos(\hat{\theta}_n - \theta_n). \quad (6)$$

In [57], [58], it is shown that given a measurement vector, $\mathbf{x}^{(n)}$, the minimum mean CE (MMCE) estimator is given by

$$\hat{\theta}_{n,\text{MMCE}}(\mathbf{x}^{(n)}) = \begin{cases} \angle E[e^{j\theta_n} | \mathbf{x}^{(n)}], & E[e^{j\theta_n} | \mathbf{x}^{(n)}] \neq 0 \\ 0, & \text{otherwise} \end{cases}, \quad (7)$$

which is the posterior circular mean at time step n .

In general, optimal estimators under periodic risks cannot be analytically derived except for a few special cases, such as the estimator from (7), which is optimal under the mean CE (MCE) risk. Therefore, a grid-search method is used for their derivation. A grid-search method involves the computation of conditional expectation, as in (3) and (5), for any point on the grid. The disadvantages of a grid-search method are: (a) its accuracy depends on the chosen grid; and (b) using a dense grid can be computationally prohibitive. In [47], a method called PERF was proposed for obtaining optimal estimators under arbitrary periodic risks. This method was derived for batch data. In this paper, we extend this method to circular stochastic filtering in which the estimators can be computed recursively at each time step, based on results from the previous steps and the new measurement. In the following section, we first review the PERF method. Then, we describe the SB-SFRF and FB-SFRF methods that utilize the PERF approach and obtain estimators under a general periodic risk in a dynamic setting.

3. SB-SFRF AND FB-SFRF METHODS

3.1. Review—PERF method

In circular stochastic filtering, our goal is minimization of an arbitrary periodic risk at each time step. First, we discuss periodic risks, whose corresponding cost function can be represented by a finite Fourier series. We refer to the case of infinite Fourier series in Subsection 3.4.

Let $C : \Omega_\varepsilon \rightarrow \mathbb{R}$ be a real, 2π -periodic, and even cost function, where $\Omega_\varepsilon \triangleq (-2\pi, 2\pi)$, that can be expressed as the following finite Fourier series [61]:

$$C(\hat{\theta}_n - \theta_n) = \sum_{k=-K}^K c_k e^{jk(\hat{\theta}_n - \theta_n)}, \quad (8)$$

for any $n = 1, 2, \dots$, where c_k , $k = -K, \dots, K$, are the corresponding Fourier coefficients of C . Since C is even, its Fourier coefficients satisfy $c_k = c_{-k}$. Given $\mathbf{x}^{(n)}$, the estimator that minimizes the Bayes risk, $E[C(\hat{\theta}_n - \theta_n)]$, is obtained by minimization of the conditional expectation

$$Q(e^{j\hat{\theta}_n}) \triangleq E[C(\hat{\theta}_n - \theta_n) | \mathbf{x}^{(n)}]. \quad (9)$$

By substituting (8) in (9) and using the linearity of the expectation operator, one obtains

$$\begin{aligned} Q(e^{j\hat{\theta}_n}) &= E \left[\sum_{k=-K}^K c_k e^{jk(\hat{\theta}_n - \theta_n)} | \mathbf{x}^{(n)} \right] \\ &= \sum_{k=-K}^K c_k m_{-k}^{(n)}(\mathbf{x}^{(n)}) e^{jk\hat{\theta}_n}, \end{aligned} \quad (10)$$

where

$$m_k^{(n)}(\mathbf{x}) \triangleq E[e^{jk\theta_n} | \mathbf{x}] \quad (11)$$

is the k th trigonometric moment of $f_{\theta_n|\mathbf{x}}$ (see e.g. [14, p. 26], [32, pp. 28–29]), where \mathbf{x} is a random vector. The term in (11) can be interpreted as a sample of the conditional characteristic function of θ_n given \mathbf{x} at an integer k . Since $f_{\theta_n|\mathbf{x}^{(n)}}$ is a real pdf, it can be verified that $m_0^{(n)}(\mathbf{x}^{(n)}) = 1$ and $m_k^{(n)}(\mathbf{x}^{(n)}) = (m_{-k}^{(n)}(\mathbf{x}^{(n)}))^*$, $k = 1, \dots, K$.

In order to obtain the estimator that minimizes $Q(e^{j\hat{\theta}_n})$ from (10), we first find stationary points of $Q(e^{j\hat{\theta}_n})$ and then find the minimum point from the set of stationary points. Since $Q(e^{j\hat{\theta}_n})$ is a real, smooth, and 2π -periodic function w.r.t. $\hat{\theta}_n$, it can be verified by using Rolle's theorem (see e.g. [54, p. 132]) that it has at least two stationary points in Ω_θ . The stationary points are obtained by equating the derivative of $Q(e^{j\hat{\theta}_n})$ w.r.t. $\hat{\theta}_n$ to zero, which yields

$$\sum_{k=-K}^K kc_k m_{-k}^{(n)}(\mathbf{x}^{(n)}) e^{jk\bar{\theta}_n} = 0, \quad (12)$$

where $\bar{\theta}_n$ is a stationary point of $Q(e^{j\hat{\theta}_n})$. In general, (12) cannot be analytically solved. Finding the stationary points and consequently the minimum point of $Q(e^{j\hat{\theta}_n})$ can be obtained by a grid-search method, whose drawbacks are discussed in Section 2. An alternative approach is utilizing the PERF method [47].

In the PERF method, the term $e^{j\hat{\theta}_n}$ in (12) is replaced by a general complex scalar $z \in \mathbb{C}$, resulting in

$$\sum_{k=-K}^K kc_k m_{-k}^{(n)}(\mathbf{x}^{(n)}) z^k = 0. \quad (13)$$

Then, a polynomial root-finding algorithm is applied on (13) and the $2K$ roots of (13), $\bar{z}_1, \dots, \bar{z}_{2K}$, are obtained. Finally, the optimal estimator is obtained by computing

$$\hat{\theta}_{n,\text{opt}} = \angle \bar{z}_{\text{opt}} = \arg \min_{\hat{\theta}_n \in \{\bar{\theta}_{n,1}, \dots, \bar{\theta}_{n,2K}\}} Q(e^{j\hat{\theta}_n}), \quad (14)$$

TABLE I
PERF method

Initialization:

- Choose a real, 2π -periodic, and even cost function, C , with Fourier series order K .
- Compute $\{c_k\}_{k=0}^K$, the Fourier coefficients of the periodic cost function C .

Algorithm stages:

- Compute $\{m_k^{(n)}(\mathbf{x}^{(n)})\}_{k=1}^K$, the trigonometric moments of $f_{\theta_n|\mathbf{x}^{(n)}}$, as defined in (11).
- Find the roots of (13), $\bar{z}_1, \dots, \bar{z}_{2K}$, and compute their corresponding phases, $\bar{\theta}_{n,1}, \dots, \bar{\theta}_{n,2K}$, respectively.
- Find $\hat{\theta}_{n,\text{opt}}$ using (10) and (14).

where $\bar{\theta}_{n,1} = \angle \bar{z}_1, \dots, \bar{\theta}_{n,2K} = \angle \bar{z}_{2K}$. It should be noted that as opposed to a grid-search method, which involves the computation of conditional expectation for any point on the grid (as mentioned in Section 2), the PERF method involves the computation of only K conditional expectations for derivation of the trigonometric moments in (11). The PERF method is summarized in Table I.

It can be seen that in order to use the PERF method in a circular stochastic filtering problem, the trigonometric moments, $\{m_k^{(n)}(\mathbf{x}^{(n)})\}_{k=1}^K$, from (11) should be computed at each time step. The SB-SFRF and FB-SFRF methods, derived in the following, enable the implementation of PERF method in a dynamic setting.

3.2. SB-SFRF method

In this subsection, we describe SB-SFRF method that can be implemented by using any sample-based filter. A sample-based filter, such as discrete filter and particle filter [2], approximates the n th step posterior pdf, $f_{\theta_n|\mathbf{x}^{(n)}}$, with a finite sum of weighted Dirac components, $f_{n,\text{SB}}^{(S)}: \Omega_\theta \rightarrow \mathbb{R}$, given by

$$f_{n,\text{SB}}^{(S)}(y) \triangleq \sum_{s=1}^S \omega_{n,s} \delta(y - \beta_{n,s}), \quad (15)$$

where y is the argument of $f_{n,\text{SB}}^{(S)}$, S is the number of samples, δ is the Dirac delta function, $\beta_{n,1}, \dots, \beta_{n,S} \in \Omega_\theta$ are the Dirac positions, and $\omega_{n,1}, \dots, \omega_{n,S}$ are nonnegative weights. The values of S , $\{\beta_{n,s}\}_{s=1}^S$, and $\{\omega_{n,s}\}_{s=1}^S$ depend on the chosen sample-based filter. In order to apply the PERF method, the first K trigonometric moments $m_1^{(n)}(\mathbf{x}^{(n)}), \dots, m_K^{(n)}(\mathbf{x}^{(n)})$ should be computed at each time step. By substituting the pdf approximation from (15) in (11), the approximations of the trigonometric moments, $\{m_k^{(n)}(\mathbf{x}^{(n)})\}_{k=1}^K$, are

$$m_{k,\text{SB}}^{(n,S)} = \sum_{s=1}^S \omega_{n,s} e^{jk\beta_{n,s}}, \quad \forall k = 1, \dots, K. \quad (16)$$

Thus, by substituting (16) in (10) and (13), the PERF method can be applied to obtain an approximation for the optimal estimator. We denote the resulting estimator

TABLE II
SB-SFRF method

Initialization:

- Choose a real, 2π -periodic, and even cost function, C , with Fourier series order K .
- Compute $\{c_k\}_{k=0}^K$, the Fourier coefficients of the periodic cost function C .

Algorithm stages for the n th time step:

- Compute the Dirac positions, $\beta_{n,1}, \dots, \beta_{n,S} \in \Omega_\theta$, and the weights, $\omega_{n,1}, \dots, \omega_{n,S}$, of the approximated posterior pdf, $f_{n,SB}^{(S)}$, from (15) by using a sample-based filter.
- Compute the approximated trigonometric moments, $m_{k,SB}^{(n,S)}$, $k = 1, \dots, K$, according to (16).
- Find the roots of (13), $\tilde{z}_1, \dots, \tilde{z}_{2K}$, and compute their corresponding phases, $\tilde{\theta}_{n,1}, \dots, \tilde{\theta}_{n,2K}$, respectively.
- Find $\hat{\theta}_{n,SB}^{(S)}$ using (10) and (14).

as $\hat{\theta}_{n,SB}^{(S)}$. The complete SB-SFRF method at time step n is summarized in Table II.

3.3. FB-SFRF method

In this subsection, we describe the FB-SFRF method that is implemented by using a Fourier-based circular filter, denoted as Fourier filter, which is proposed in [44]. First, we define

$$f_{\theta_0}^{(p)}(\alpha_0) \triangleq \sum_{l=-\infty}^{\infty} f_{\theta_0}(\alpha_0 + 2\pi l) \quad (17)$$

and for any $n = 1, 2, \dots$,

$$f_{\theta_n|\theta_{n-1}}^{(p)}(\alpha_n | \alpha_{n-1}) \triangleq \sum_{l=-\infty}^{\infty} \sum_{m=-\infty}^{\infty} f_{\theta_n|\theta_{n-1}}(\alpha_n + 2\pi l | \alpha_{n-1} + 2\pi m), \quad (18)$$

$$f_{\mathbf{x}_n|\theta_n}^{(p)}(\beta_n | \alpha_n) \triangleq \sum_{l=-\infty}^{\infty} f_{\mathbf{x}_n|\theta_n}(\beta_n | \alpha_n + 2\pi l), \quad (19)$$

$$f_{\theta_n|\mathbf{x}^{(n)}}^{(p)}(\alpha_n | \beta^{(n)}) \triangleq \sum_{l=-\infty}^{\infty} f_{\theta_n|\mathbf{x}^{(n)}}(\alpha_n + 2\pi l | \beta^{(n)}), \quad (20)$$

$$f_{\theta_n|\mathbf{x}^{(n-1)}}^{(p)}(\alpha_n | \beta^{(n-1)}) \triangleq \sum_{l=-\infty}^{\infty} f_{\theta_n|\mathbf{x}^{(n-1)}}(\alpha_n + 2\pi l | \beta^{(n-1)}), \quad (21)$$

which are the 2π -periodic extensions of the pdfs f_{θ_0} , $f_{\theta_n|\theta_{n-1}}$, $f_{\mathbf{x}_n|\theta_n}$, $f_{\theta_n|\mathbf{x}^{(n)}}$, and $f_{\theta_n|\mathbf{x}^{(n-1)}}$, respectively, w.r.t. $\{\theta_n\}_{n \geq 0}$.

Since $f_{\theta_0}^{(p)}$ is a 2π -periodic function w.r.t. θ_0 and since $f_{\mathbf{x}_n|\theta_n}^{(p)}$, $f_{\theta_n|\mathbf{x}^{(n)}}$, and $f_{\theta_n|\mathbf{x}^{(n-1)}}$ are 2π -periodic functions w.r.t. θ_n , it is assumed that they can be represented via Fourier series with Fourier coefficients $\{\eta_l^{(0)}\}_{l \in \mathbb{Z}}$, $\{d_l^{(n)}(\mathbf{x}_n)\}_{l \in \mathbb{Z}}$, $\{\eta_l^{(n|n)}(\mathbf{x}^{(n)})\}_{l \in \mathbb{Z}}$, and $\{\eta_l^{(n|n-1)}(\mathbf{x}^{(n-1)})\}_{l \in \mathbb{Z}}$, respectively. That is,

$$f_{\theta_0}^{(p)}(\alpha_0) = \sum_{l=-\infty}^{\infty} \eta_l^{(0)} e^{jl\alpha_0}, \quad (22)$$

$$f_{\mathbf{x}_n|\theta_n}^{(p)}(\beta_n | \alpha_n) = \sum_{l=-\infty}^{\infty} d_l^{(n)}(\beta_n) e^{jl\alpha_n}, \quad (23)$$

$$f_{\theta_n|\mathbf{x}^{(n)}}^{(p)}(\alpha_n | \beta^{(n)}) = \sum_{l=-\infty}^{\infty} \eta_l^{(n|n)}(\beta^{(n)}) e^{jl\alpha_n}, \quad (24)$$

and

$$f_{\theta_n|\mathbf{x}^{(n-1)}}^{(p)}(\alpha_n | \beta^{(n-1)}) = \sum_{l=-\infty}^{\infty} \eta_l^{(n|n-1)}(\beta^{(n-1)}) e^{jl\alpha_n}. \quad (25)$$

Similarly, the function $f_{\theta_n|\theta_{n-1}}^{(p)}$ is a 2π -periodic function w.r.t. both θ_n and θ_{n-1} , and therefore, it is assumed that it can be represented via a two-dimensional Fourier series with Fourier coefficients $\{\phi_{l,m}^{(n)}\}_{l,m \in \mathbb{Z}}$, i.e.

$$f_{\theta_n|\theta_{n-1}}^{(p)}(\alpha_n | \alpha_{n-1}) = \sum_{l=-\infty}^{\infty} \sum_{m=-\infty}^{\infty} \phi_{l,m}^{(n)} e^{jl\alpha_n} e^{jm\alpha_{n-1}}. \quad (26)$$

Based on the Fourier-based filters proposed in [7], [44], [57], [58], we derive prediction and update stages, which are applied on the Fourier coefficients of $f_{\theta_n|\mathbf{x}^{(n)}}$ and $f_{\theta_n|\mathbf{x}^{(n-1)}}$.

• Prediction:

According to Chapman-Kolmogorov equation and by using the Markovian nature of the state model in (1), the predicted pdf $f_{\theta_n|\mathbf{x}^{(n-1)}}$ is given by (see e.g. [2, Eq. (3)])

$$f_{\theta_n|\mathbf{x}^{(n-1)}}(\alpha_n | \beta^{(n-1)}) = \int_{\Omega_\theta} f_{\theta_n|\theta_{n-1}}(\alpha_n | \alpha_{n-1}) \times f_{\theta_{n-1}|\mathbf{x}^{(n-1)}}(\alpha_{n-1} | \beta^{(n-1)}) d\alpha_{n-1}, \quad \forall \alpha_n \in \Omega_\theta. \quad (27)$$

For $\theta_n, \theta_{n-1} \in \Omega_\theta$, the pdfs in the left hand side (l.h.s.) and right hand side (r.h.s.) of (27) are equal to their periodic extensions. Thus, (27) can be rewritten as

$$f_{\theta_n|\mathbf{x}^{(n-1)}}^{(p)}(\alpha_n | \beta^{(n-1)}) = \int_{\Omega_\theta} f_{\theta_n|\theta_{n-1}}^{(p)}(\alpha_n | \alpha_{n-1}) \times f_{\theta_{n-1}|\mathbf{x}^{(n-1)}}^{(p)}(\alpha_{n-1} | \beta^{(n-1)}) d\alpha_{n-1}, \quad \forall \alpha_n \in \Omega_\theta. \quad (28)$$

By substituting the corresponding Fourier series from (22), (24), and (26) in the r.h.s. of (28), we obtain the Fourier series representation of $f_{\theta_n|\mathbf{x}^{(n-1)}}$ from (25), whose l th Fourier coefficient is given by [7]

$$\eta_l^{(n|n-1)}(\mathbf{x}^{(n-1)}) = 2\pi \sum_{m=-\infty}^{\infty} \eta_{-m}^{(n-1|n-1)}(\mathbf{x}^{(n-1)}) \phi_{l,m}^{(n)}, \quad (29)$$

$\forall l \in \mathbb{Z}$, $n = 1, 2, \dots$, where $\eta_l^{(0|0)}(\mathbf{x}^{(0)}) \triangleq \eta_l^{(0)}$.

• Update:

According to Bayes' rule, the posterior pdf $f_{\theta_n|\mathbf{x}^{(n)}}$ is given by (see e.g. [2, Eq. (4)])

$$f_{\theta_n|\mathbf{x}^{(n)}}(\alpha_n | \beta^{(n)}) = \frac{f_{\mathbf{x}_n|\theta_n}(\beta_n | \alpha_n) f_{\theta_n|\mathbf{x}^{(n-1)}}(\alpha_n | \beta^{(n-1)})}{\int_{\Omega_\theta} f_{\mathbf{x}_n|\theta_n}(\beta_n | \alpha_n) f_{\theta_n|\mathbf{x}^{(n-1)}}(\alpha_n | \beta^{(n-1)}) d\alpha_n}, \quad (30)$$

$\forall \alpha_n \in \Omega_\theta$. For $\theta_n \in \Omega_\theta$, the pdfs in the l.h.s. and r.h.s. of (30) are equal to their periodic extensions. Thus, (30) can be rewritten as

$$f_{\theta_n|\mathbf{x}^{(n)}}^{(p)}(\alpha_n | \beta^{(n)}) = \frac{f_{\mathbf{x}_n|\theta_n}^{(p)}(\beta_n | \alpha_n) f_{\theta_n|\mathbf{x}^{(n-1)}}^{(p)}(\alpha_n | \beta^{(n-1)})}{\int_{\Omega_\theta} f_{\mathbf{x}_n|\theta_n}^{(p)}(\beta_n | \alpha_n) f_{\theta_n|\mathbf{x}^{(n-1)}}^{(p)}(\alpha_n | \beta^{(n-1)}) d\alpha_n}, \quad (31)$$

$\forall \alpha_n \in \Omega_\theta$. By substituting the corresponding Fourier series from (23) and (25) in the r.h.s. of (31), we obtain the Fourier series representation of $f_{\theta_n|\mathbf{x}^{(n)}}^{(p)}$ from (24), whose l th Fourier coefficient is given by [7]

$$\eta_l^{(n|n)}(\mathbf{x}^{(n)}) = \frac{\gamma_l^{(n)}(\mathbf{x}^{(n)})}{2\pi\gamma_0^{(n)}(\mathbf{x}^{(n)})}, \quad (32)$$

$\forall l \in \mathbb{Z}$, $n = 1, 2, \dots$, where

$$\gamma_l^{(n)}(\mathbf{x}^{(n)}) \triangleq \sum_{m=-\infty}^{\infty} \eta_m^{(n|n-1)}(\mathbf{x}^{(n-1)}) d_{l-m}^{(n)}(\mathbf{x}_n).$$

Since $f_{\theta_n|\mathbf{x}^{(n)}}$ from (30) is equal to $f_{\theta_n|\mathbf{x}^{(n)}}^{(p)}$ from (31) for $\theta_n \in \Omega_\theta$, the Fourier series of $f_{\theta_n|\mathbf{x}^{(n)}}^{(p)}$ can be used to represent $f_{\theta_n|\mathbf{x}^{(n)}}$. In practice, $f_{\theta_n|\mathbf{x}^{(n)}}$ is approximated by a finite Fourier series, $f_{n,\text{FB}}^{(D)} : \Omega_\theta \rightarrow \mathbb{R}$, given by

$$f_{n,\text{FB}}^{(D)}(y) \triangleq \sum_{l=-D}^D \eta_{l,\text{FB}}^{(n,D)} e^{jly}, \quad (33)$$

where y is the argument of $f_{n,\text{FB}}^{(D)}$ and D is the chosen Fourier series order. The series order, D , is determined by taking into account the trade-off between estimation quality and required rate of convergence. The approximation accuracy, i.e. the distance between the actual pdf and its Fourier series approximation, can be measured for example by using Hellinger metric [7] or Kullback-Leibler divergence [44]. At time step n , $\eta_{l,\text{FB}}^{(n,D)}$ approximates $\eta_l^{(n|n)}(\mathbf{x}^{(n)})$, $\forall l = -D, \dots, D$, and for $|l| > D$, $\eta_l^{(n|n)}(\mathbf{x}^{(n)})$ is approximated by zero. The Fourier series approximation of $f_{\theta_n|\mathbf{x}^{(n)}}$ in (33) represents a pdf and thus, should be nonnegative and integrate to 1. In order to maintain the approximation in (33) as a valid pdf, the approach in [44] that approximates $\sqrt{f_{\theta_n|\mathbf{x}^{(n)}}}$ by a finite Fourier series, is applied. It should be noted that it is assumed in [44] that $f_{\theta_n|\theta_{n-1}}^{(p)}(\alpha_n | \alpha_{n-1}) = g(\alpha_n - \alpha_{n-1})$, $\forall \alpha_n, \alpha_{n-1} \in \Omega_\theta$, for some function g , which simplifies the prediction stage. An explanation is added in the appendix for implementing the prediction stage, under the approach of [44], with a general $f_{\theta_n|\theta_{n-1}}^{(p)}$.

By substituting the pdf approximation from (33) in (11) and since $\int_{\Omega_\theta} e^{jl\alpha} d\alpha = 2\pi\delta_{\text{kr}}(l)$, where δ_{kr} is the Kronecker delta function, the approximations of the trigonometric moments, $\{m_k^{(n)}(\mathbf{x}^{(n)})\}_{k=1}^K$, are

$$m_{k,\text{FB}}^{(n,D)} = 2\pi\eta_{-k,\text{FB}}^{(n,D)}, \quad \forall k = 1, \dots, K. \quad (34)$$

TABLE III
FB-SFRF method

Initialization:

- Choose a real, 2π -periodic, and even cost function, C , with Fourier series order K .
- Compute $\{c_k\}_{k=0}^K$, the Fourier coefficients of the periodic cost function C .

Algorithm stages for the n th time step:

- Compute the Fourier coefficients, $\eta_{l,\text{FB}}^{(n,D)}$, $l = 1, \dots, D$, of the approximated posterior pdf, $f_{n,\text{FB}}^{(D)}$, from (33) by using the Fourier-based circular filter from [44].
- Compute the approximated trigonometric moments, $m_{k,\text{FB}}^{(n,D)}$, $k = 1, \dots, K$, according to (34).
- Find the roots of (13), $\tilde{z}_1, \dots, \tilde{z}_{2K}$, and compute their corresponding phases, $\tilde{\theta}_{n,1}, \dots, \tilde{\theta}_{n,2K}$, respectively.
- Find $\hat{\theta}_{n,\text{FB}}^{(D)}$ using (10) and (14).

In case $K > D$, then $m_{k,\text{FB}}^{(n,D)} = 0$, $\forall k = D + 1, \dots, K$. Thus, by substituting (34) in (10) and (13), the PERF method can be applied to obtain an approximation for the optimal estimator. We denote the resulting estimator as $\hat{\theta}_{n,\text{FB}}^{(D)}$. The complete FB-SFRF method at time step n is summarized in Table III.

3.4. SB-SFRF and FB-SFRF methods with a general periodic cost function

Consider a 2π -periodic cost function, C , with a convergent infinite Fourier series representation. It is shown in [47] that under some regularity conditions, PERF method, applied on a truncated Fourier series representation of C with $K < \infty$, converges to the corresponding optimal estimator in the limit $K \rightarrow \infty$. For such cost functions the SB-SFRF and FB-SFRF methods are applied on a truncated Fourier series.

In the following, we describe three examples for periodic risks, the mean SPE (MSPE), mean APE (MAPE), and MCE risks and discuss the implementation of SB-SFRF and FB-SFRF methods under these risks. In order to apply SB-SFRF and FB-SFRF methods with the MSPE, MAPE, and MCE risks, their corresponding Fourier coefficients should be computed. The Fourier series order of the CE cost function is $K = 1$ and SB-SFRF and FB-SFRF methods can be directly applied. As opposed to the CE cost function, the Fourier series of the SPE and APE cost functions are infinite and therefore, SB-SFRF and FB-SFRF methods are applied on their truncated Fourier series representations. It is shown in [47] that under mild conditions PERF method converges to the optimal estimators under the MSPE and MAPE risks in the limit $K \rightarrow \infty$, which justifies applying SB-SFRF and FB-SFRF methods under these risks. The Fourier series, Fourier coefficients, and explicit form of (13) for the SPE, APE, and CE cost functions, are presented in Table IV.

It is shown in [47] that the optimal estimator under first-order Fourier series approximation of the SPE and the APE cost functions, i.e. for choosing $K = 1$, is given

TABLE IV
The Fourier series of the cost functions

Cost function	Squared periodic error (SPE)	Absolute periodic error (APE)	Cyclic error (CE)
Fourier series of $C(\varepsilon)$	$\frac{\pi^2}{3} + 2 \sum_{k \in \mathbb{Z}, k \neq 0} \frac{(-1)^k}{k^2} e^{jk\varepsilon}$	$\frac{\pi}{2} - 2 \sum_{k \in \mathbb{Z}} \frac{1}{\pi(2k+1)^2} e^{i(2k+1)\varepsilon}$	$2 - e^{j\varepsilon} - e^{-j\varepsilon}$
Fourier coefficients c_k	$\begin{cases} \frac{\pi^2}{3}, & k = 0 \\ \frac{2(-1)^k}{k^2}, & k \neq 0 \end{cases}$	$\begin{cases} \frac{\pi}{2}, & k = 0 \\ 0, & k \neq 0 \text{ and even} \\ -\frac{2}{\pi k^2}, & k \text{ odd} \end{cases}$	$\begin{cases} 2, & k = 0 \\ -1, & k = \pm 1 \\ 0, & \text{otherwise} \end{cases}$
Explicit form of (13) at n th time step	$\sum_{k=-K, k \neq 0}^K \frac{(-1)^k m_{-k}^{(n)}(\mathbf{x}^{(n)})}{k} z^k = 0$	$\sum_{k=-\lfloor (K+1)/2 \rfloor}^{\lfloor (K-1)/2 \rfloor} \frac{m_{-2k-1}^{(n)}(\mathbf{x}^{(n)})}{2k+1} z^{2k} = 0$	$m_{-1}^{(n)}(\mathbf{x}^{(n)})z + m_1^{(n)}(\mathbf{x}^{(n)})z^{-1} = 0$

by the posterior circular mean estimator, which is the MMCE estimator from (7). In addition, it is shown in [47] and [30] that the posterior circular mean estimator is optimal under the MSPE and MAPE risks, in case the posterior pdf is unimodal and even (as a function supported on the circle). In the general case, where the posterior pdf is not necessarily unimodal and even, choosing $K > 1$ for the SPE and APE approximations and applying SB-SFRF or FB-SFRF methods can improve the performance, comparing to the posterior circular mean estimator, under the MSPE and MAPE risks. We denote SB-SFRF and FB-SFRF methods under the MSPE risk as SB-SFRF-MSPE and FB-SFRF-MSPE, respectively. Similarly, SB-SFRF and FB-SFRF methods under the MAPE risk are denoted by SB-SFRF-MAPE and FB-SFRF-MAPE, respectively.

Remarks:

- 1) *Periodic cost functions:* In the conventional Bayesian framework, the SE and absolute-error (AE) cost functions are commonly used for performance evaluation. One of the differences between these cost functions is that the SE increases faster than the AE and thus, the SE is more sensitive to outliers [25, p. 51]. The SPE and APE are the natural periodic equivalents of the SE and AE, respectively. They are obtained by periodically extending their conventional counterparts. The CE can be viewed as a smooth first order approximation, in terms of Fourier series, of the SPE and APE [47]. In the small error region, the APE and SPE coincide with the AE and SE, respectively. Similar to the SPE, in the small error region, the CE coincides with the SE.
- 2) *Computational complexity:* The additional run-time complexity induced from using SB-SFRF and FB-SFRF methods with $K > 1$ series order is dominated by the polynomial root-finding applied on (13). Since the order of the polynomial in (13) is limited by $2K$, the additional run-time at each time step is of the order $O(K^3)$ [47]. The prediction and update stages of SB-SFRF and FB-SFRF methods

are mainly affected by the chosen filter and chosen number of samples/Fourier coefficients that are used for approximating the posterior pdf. For FB-SFRF method, the asymptotic run-time complexity of both the prediction and update stages of the Fourier filter is $O(D \log D)$ [44], where D is the chosen Fourier series order of the approximated posterior pdf in (33). For SB-SFRF method, the asymptotic run-time complexity depends on the complexity of the chosen sample-based filter.

- 3) *Choosing the value of K :* In general, for periodic cost functions with infinite Fourier series, the value of K can be determined by taking into account the trade-off between the additional computational complexity, induced from using SB-SFRF and FB-SFRF methods, and the accuracy of approximating the cost function Fourier series with a finite K . In addition, the performance improvement with a larger K depends on the posterior pdf approximation accuracy. The periodic cost functions approximation error can be assessed by using Parseval's formula [61, pp. 12–13].

4. EXAMPLE—DOA TRACKING

In this section, we consider the problem of single source DOA tracking by using a uniform circular array (UCA). At time step n , the measurement at the l th sensor is modeled as (see e.g. [43])

$$x_{n,l} = \xi e^{j\zeta \cos(\theta_n - (2\pi l/L))} + \nu_{n,l}, \quad l = 1, \dots, L. \quad (35)$$

where ξ is the signal complex amplitude, which is assumed to be known, $\zeta = 2\pi r/\lambda$, where r is the UCA radius and λ is the signal wavelength, θ_n is the signal DOA, and $\{\nu_n\}$ is an independent identically distributed (i.i.d.) complex circularly symmetric zero mean Gaussian noise vector sequence with known covariance matrix $\sigma^2 \mathbf{I}_L$, where \mathbf{I}_L is the identity matrix of size L . The DOA state model is given by

$$\theta_n = [\theta_{n-1} + w_n]_{2\pi}, \quad (36)$$

where $\{w_n\}$ is an i.i.d. noise in which each element is distributed according to a mixture of two von Mises distributions [14], [32] with known circular means μ_1, μ_2 and concentration parameters κ_1, κ_2 , i.e.

$$f_{w_n}(v) = \begin{cases} \epsilon \frac{e^{\kappa_1 \cos(v-\mu_1)}}{2\pi I_0(\kappa_1)} + (1-\epsilon) \frac{e^{\kappa_2 \cos(v-\mu_2)}}{2\pi I_0(\kappa_2)}, & v \in [-\pi, \pi) \\ 0, & \text{otherwise} \end{cases}, \quad (37)$$

where I_m is the modified Bessel function of order m and $0 \leq \epsilon \leq 1$ is a parameter that determines the weights between the two von Mises distributions. The 2π -periodic extension of f_{w_n} w.r.t. w_n is given by

$$f_{w_n}^{(p)}(v) = \epsilon \frac{e^{\kappa_1 \cos(v-\mu_1)}}{2\pi I_0(\kappa_1)} + (1-\epsilon) \frac{e^{\kappa_2 \cos(v-\mu_2)}}{2\pi I_0(\kappa_2)}, \quad \forall v \in \mathbb{R}.$$

The von Mises distribution is one of the most popular distributions for modeling random parameters with circular nature and is analogous to the Gaussian distribution on the real axis (see e.g. [11], [14], [32], [60]). Many noncircular distributions can be approximated to any desired degree of approximation in terms of Kullback-Leibler divergence, using a finite mixture of Gaussian distributions [19], [27], [46], [52]. Similarly, it is claimed in [32, p. 90] that some circular distributions are fitted well by mixtures of von Mises distributions. In [9] and [34], mixtures of von Mises distributions are used for modeling multimodal distributions on the circle. Multimodal state noise is considered e.g. in [6], [18], [28] for modeling abrupt changes in the state. It is assumed that the sequences $\{w_n\}$ and $\{\nu_n\}$ are statistically independent as well as independent of past and present states. In addition, it is assumed that the prior distribution of θ_0 is uniform, i.e. $\theta_0 \sim U(-\pi, \pi)$. Under this model, the Fourier coefficients of $f_{\theta_0}^{(p)}$ and $f_{\theta_n|\theta_{n-1}}^{(p)}$ are given by

$$\eta_l^{(0)} = \begin{cases} \frac{1}{2\pi}, & l = 0 \\ 0, & \text{otherwise} \end{cases} \quad (38)$$

and

$$\phi_{l,m}^{(n)} = \left(\epsilon \frac{I_{|l|}(\kappa_1)}{2\pi I_0(\kappa_1)} e^{-jl\mu_1} + (1-\epsilon) \frac{I_{|l|}(\kappa_2)}{2\pi I_0(\kappa_2)} e^{-jl\mu_2} \right) \delta_{\text{kr}}(l+m), \quad (39)$$

$\forall l, m \in \mathbb{Z}$, $n = 1, 2, \dots$, respectively. In this case, $f_{\theta_n|\theta_{n-1}}^{(p)}(\alpha_n | \alpha_{n-1}) = f_{w_n}^{(p)}(\alpha_n - \alpha_{n-1})$, $\forall \alpha_n, \alpha_{n-1} \in \Omega_\theta$, which simplifies the prediction stage. As proposed in [44], the Fourier coefficients of $f_{x_n|\theta_n}$ are approximated using the fast Fourier transform [42].

For this problem, the SB-SFRF and FB-SFRF methods are implemented under the MSPE and MAPE risks. For computation of the approximated trigonometric moments in SB-SFRF method, the particle filter from [2]

with the state transition pdf as importance function, is used. The root-finding step is employed by the function ‘roots’ of Matlab.

The SB-SFRF method is implemented with $S = 500$ samples (particles in this case) and the FB-SFRF method is implemented with $D = 40$ Fourier coefficients. In addition, we assume $L = 4$, $\zeta = 10$, $\sigma^2 = 1$, $\mu_1 = 0.95\pi$, $\kappa_1 = 20$, $\mu_2 = 0$, $\kappa_2 = 10$, $\epsilon = 0.5$, and $\xi = (1/\sqrt{2}) + j(1/\sqrt{2})$. The MSPEs and MAPEs of the considered methods are evaluated using 10,000 Monte-Carlo trials. In the following, the posterior mean estimator obtained by particle filter is denoted as Particle-PM. The posterior circular mean estimators obtained by particle and Fourier filters are denoted as Particle-CM and Fourier-CM, respectively. The proposed SB-SFRF-MSPE and SB-SFRF-MAPE methods implemented with particle filter are denoted as Particle-SB-SFRF-MSPE and Particle-SB-SFRF-MAPE, respectively.

In Figs. 2–3, the MSPEs of particle and Fourier estimators are presented versus the time step n , where the corresponding SB-SFRF and FB-SFRF methods are evaluated with $K = 2, 12$. It should be noted that for $K = 1$, the proposed Particle-SB-SFRF-MSPE and FB-SFRF-MSPE methods coincide with the Particle-CM and Fourier-CM, respectively. It can be seen that in both cases, the proposed SFRF-MSPE methods with $K = 12$ result in lower MSPEs than with $K = 2$ and that SFRF-MSPE methods with $K = 2, 12$ have lower MSPEs than the MSPEs of the posterior mean and posterior circular mean estimators.

Figs. 4–5 show the MSPEs of Particle-SB-SFRF-MSPE and FB-SFRF-MSPE methods as a function of the series order, K , averaged over all time steps $n = 1, \dots, 30$. It can be seen that in both cases, the MSPE decreases as K increases. The non-monotonic decrease can be explained by the fact that the error is evaluated w.r.t. the actual periodic cost function, while the minimization is w.r.t. its truncated approximation, which suffers from inaccuracies due to, for example, Gibbs phenomenon [61]. It can be seen that for Particle-SB-SFRF-MSPE and FB-SFRF-MSPE, the MSPEs with $K = 20$ are lower than the MSPEs with $K = 1$ by approximately 16.4% and 15.6%, respectively. For both methods, the MSPEs with $K \geq 5$ are very close to the MSPEs with $K = 20$. Therefore, the choice $K = 5$ seems appropriate in this case. The SPE cost function and its Fourier series approximations are depicted in Fig. 6, with series orders $K = 1, 2, 12$.

In Figs. 7–8 the MAPEs of particle and Fourier estimators are presented versus the time step n , where the corresponding SB-SFRF and FB-SFRF methods are evaluated with $K = 3, 23$. Similar to the MSPE case, for $K = 1$, the proposed Particle-SB-SFRF-MAPE and FB-SFRF-MAPE methods coincide with the Particle-CM and Fourier-CM, respectively. It can be seen that in both cases, SFRF-MAPE methods with $K = 23$ result in lower MAPEs than with $K = 3$ and that SFRF-MAPE

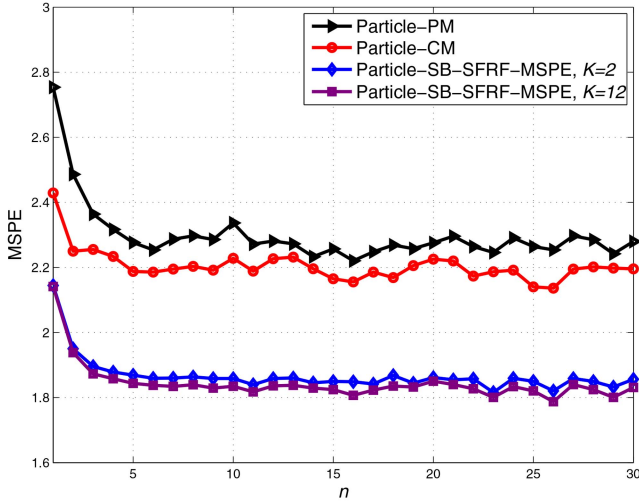


Fig. 2. The MSPEs of Particle-PM, Particle-CM, and Particle-SB-SFRF-MSPE method $K = 2, 12$, with $S = 500$ samples, versus the time step n .

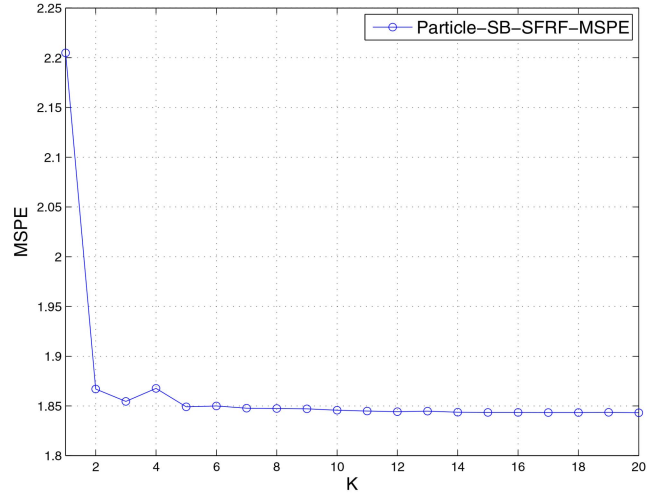


Fig. 4. The MSPE of Particle-SB-SFRF-MSPE method with $S = 500$ samples versus K , averaged over time steps $n = 1, \dots, 30$.

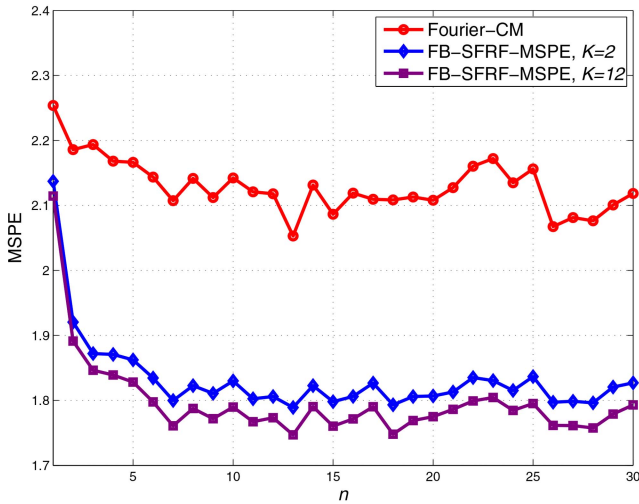


Fig. 3. The MSPEs of Fourier-CM and FB-SFRF-MSPE method $K = 2, 12$, with $D = 40$ Fourier coefficients, versus the time step n .

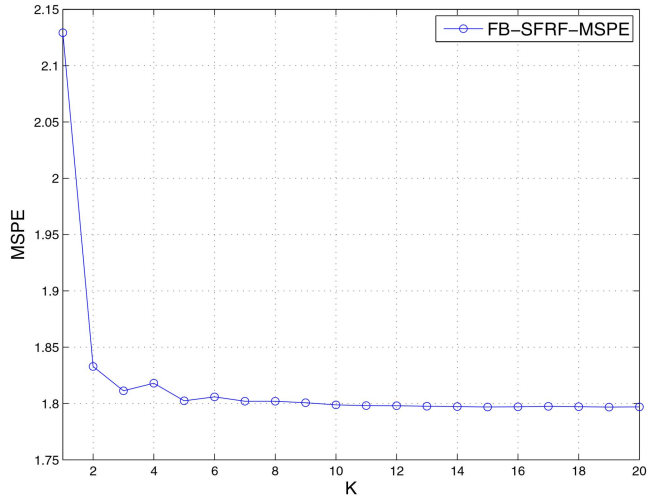


Fig. 5. The MSPE of FB-SFRF-MSPE method with $D = 40$ Fourier coefficients versus K , averaged over time steps $n = 1, \dots, 30$.

methods with $K = 3, 23$ have lower MAPEs than the MAPEs of the posterior circular mean estimators.

Figs. 9–10 show the MAPEs of Particle-SB-SFRF-MAPE and FB-SFRF-MAPE methods as a function of the series order, K , averaged over all time steps $n = 1, \dots, 30$. It can be seen that in both cases, the MAPE decreases as K increases. For Particle-SB-SFRF-MAPE and FB-SFRF-MAPE, the MAPEs with $K = 39$ are lower than the MAPEs with $K = 1$ by approximately 3.5% and 4.2%, respectively. For both methods, the MAPEs with $K \geq 9$ are very close to the MAPEs with $K = 39$. Therefore, the choice $K = 9$ seems appropriate in this case. It can be seen that the improvement in MAPE is smaller for both methods in comparison to the improvement in MSPE. The reason for this phenomenon may be that the SPE increases faster than the APE and thus, a low value of K is highly penalized by the SPE.

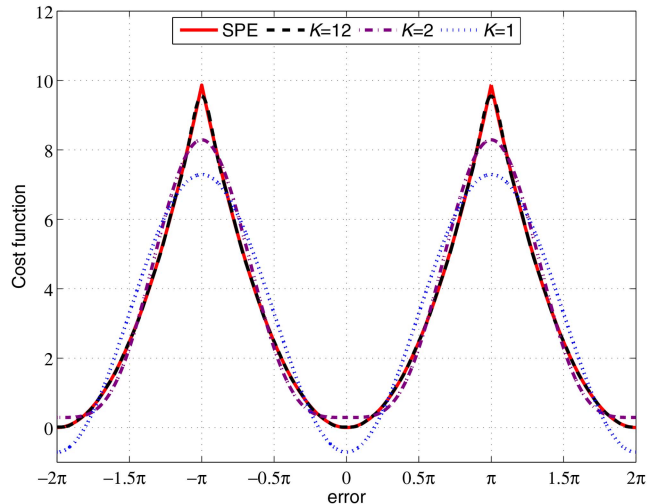


Fig. 6. Fourier series approximations of SPE with $K = 1, 2, 12$.

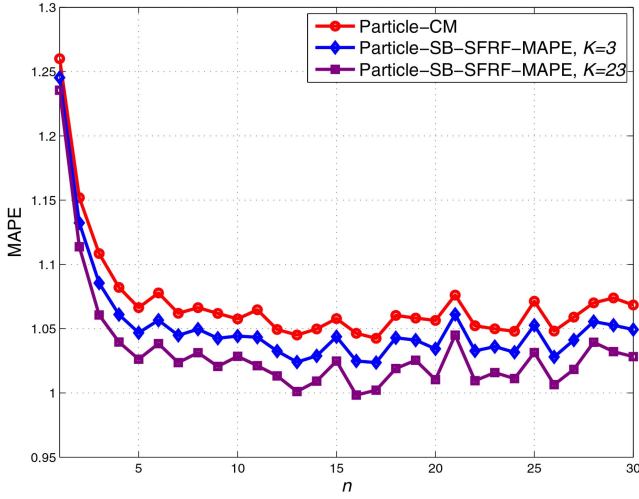


Fig. 7. The MAPEs of Particle-CM and Particle-SB-SFRF-MAPE method $K = 3, 23$, with $S = 500$ samples, versus the time step n .

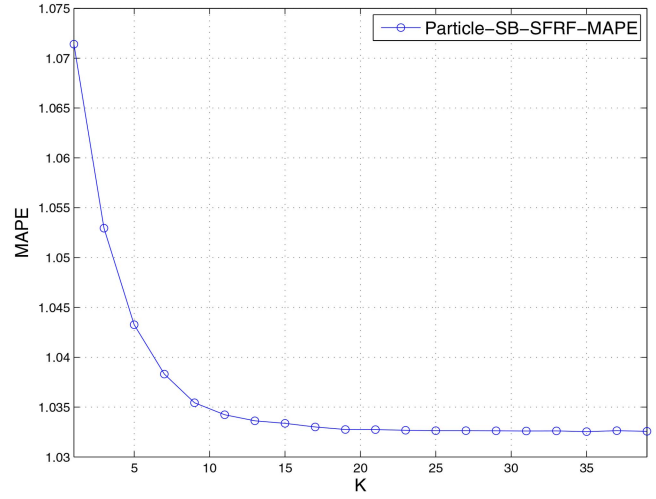


Fig. 9. The MAPE of Particle-SB-SFRF-MAPE method with $S = 500$ samples versus K , averaged over time steps $n = 1, \dots, 30$.

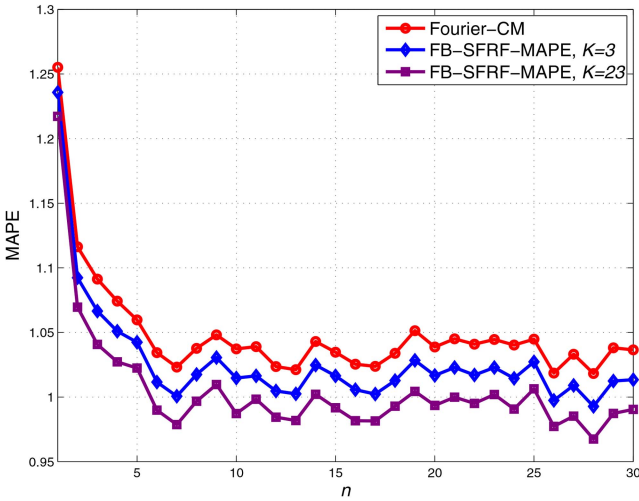


Fig. 8. The MAPEs of Fourier-CM and FB-SFRF-MAPE method $K = 3, 23$, with $D = 40$ Fourier coefficients, versus the time step n .

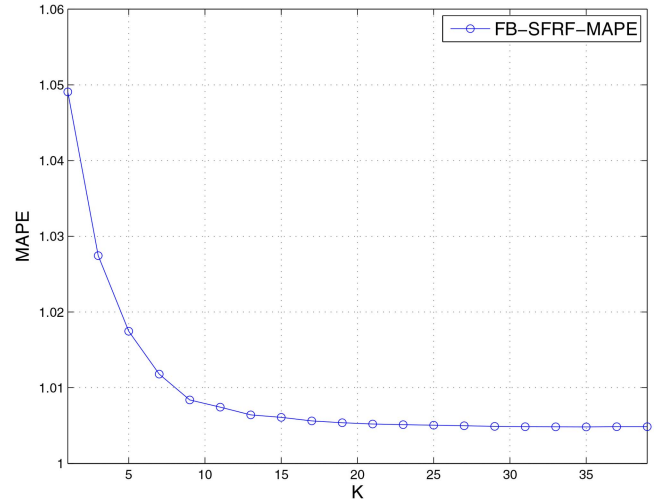


Fig. 10. The MAPE of FB-SFRF-MAPE method with $D = 40$ Fourier coefficients versus K , averaged over time steps $n = 1, \dots, 30$.

In Figs. 11–12, the MSPEs of particle and Fourier estimators are presented versus $\text{SNR} \triangleq |\xi|^2/\sigma^2$, averaged over all time steps $n = 1, \dots, 30$, where the corresponding SB-SFRF and FB-SFRF methods are evaluated with $K = 2, 12$. It can be seen that for both methods, SFRF-MSPE methods with $K = 12$ result in lower MSPEs than SFRF-MSPE methods with $K = 2$ and the corresponding posterior circular mean estimators. In addition, it can be seen that the difference between $K = 2$ and $K = 12$ is small.

As a comparison between SB-SFRF and FB-SFRF methods, we examine their performance in terms of MSPE for a similar number of samples or Fourier coefficients for the posterior pdf approximation, i.e. $S = F = 2D + 1$. In order to broaden the comparison, we implemented a discrete filter [24], used in [44], which is based on wrapped Dirac distribution. In the following, the SB-SFRF-MSPE method implemented with discrete filter is denoted as Discrete-SB-SFRF-MSPE. The

MSPEs of the considered SFRF-MSPE methods with $K = 2$, are presented in Fig. 13 versus the time step n . It can be seen that for $S = F = 9$, FB-SFRF method significantly outperforms SB-SFRF method with particle and discrete filters in all time steps. For $S = F = 201$, FB-SFRF method outperforms SB-SFRF method with particle filter in all time steps and the difference between FB-SFRF method and SB-SFRF method with discrete filter is small for $n \geq 7$. In general, in the considered scenario, the FB-SFRF method seems favourable over SB-SFRF method with both discrete and particle filters, especially in the case, in which only few samples/Fourier coefficients are available. The reason for FB-SFRF advantage may be the discrete representation of the posterior pdf in the frequency domain rather than parameter domain.

Finally, we examine the performance of SB-SFRF and FB-SFRF methods for unimodal state noise. Similar to [11], the a priori pdf of θ_0 is assumed to be a

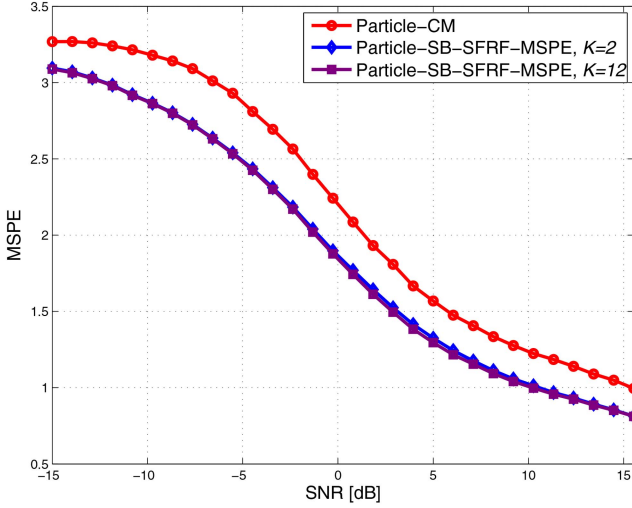


Fig. 11. The MSPEs of Particle-CM and Particle-SB-SFRF-MSPE method $K = 2, 12$, with $S = 500$ samples, versus SNR, averaged over time steps $n = 1, \dots, 30$.

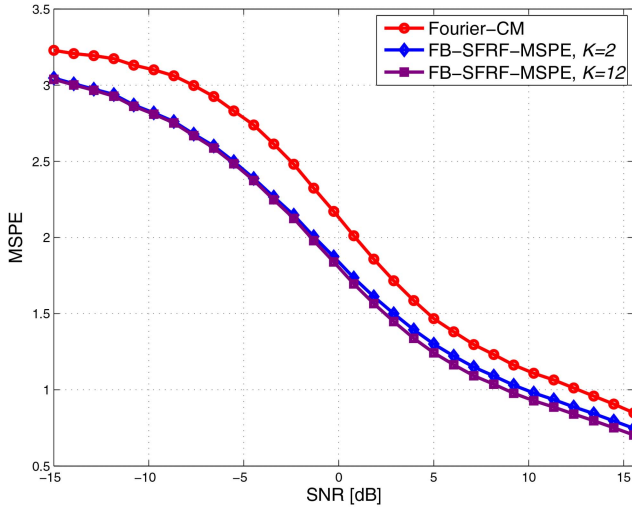


Fig. 12. The MSPEs of Fourier-CM and FB-SFRF-MSPE method $K = 2, 12$, with $D = 40$ Fourier coefficients, versus SNR, averaged over time steps $n = 1, \dots, 30$.

mixture of two von Mises distributions, as in (37), with known circular means $\mu_{0,1} = 0.21$, $\mu_{0,2} = 1.91$, concentration parameters $\kappa_{0,1} = 9$, $\kappa_{0,2} = 39$, and weighting parameter $\epsilon_0 = 0.3$. The state-space model is assumed to be as in (35) and (36), except that each state noise element is assumed to be von Mises distributed with circular mean $\mu = 0$ and concentration parameter $\kappa = 3$. In this scenario, the discrete filter is also used for implementation of SB-SFRF method. In the following, the posterior mean and posterior *circular* mean estimators obtained by discrete filter are denoted as Discrete-PM and Discrete-CM, respectively. In Figs. 14–16 the MSPEs of particle, discrete, and Fourier estimators, are presented versus the time step n , where the corresponding SB-SFRF and FB-SFRF methods are evaluated with $K = 2, 12$. It can be seen that in all cases, SFRF-MSPE methods with $K = 12$ result in lower MSPEs than with

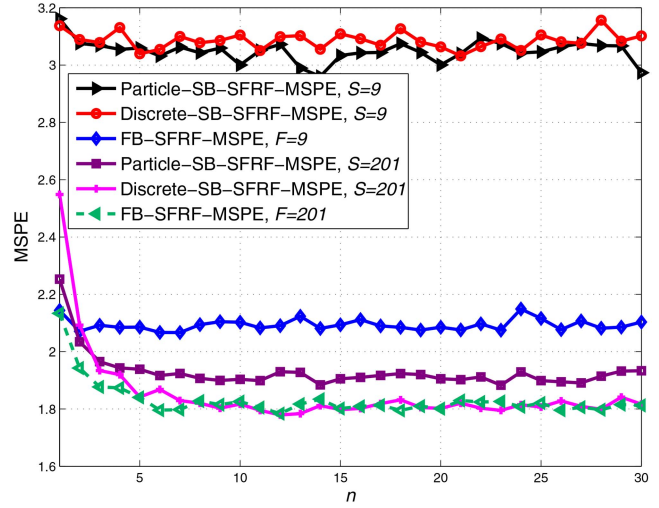


Fig. 13. The MSPEs of Particle-SB-SFRF-MSPE, Discrete-SB-SFRF-MSPE, and FB-SFRF-MSPE methods with $K = 2$, $S = F = 9$ and $S = F = 201$ samples/Fourier coefficients, versus the time step n .

$K = 2$ and that SFRF-MSPE methods with $K = 2, 12$ have lower MSPEs than the MSPEs of the posterior mean and posterior circular mean estimators.

5. CONCLUSION

In this paper, we propose two methods, SB-SFRF and FB-SFRF, for derivation of estimators under general periodic Bayes risks in circular stochastic filtering problems. Both methods utilize the PERF method [47], which is based on Fourier series representation of an arbitrary periodic cost function and polynomial root-finding. The proposed methods are not based on a grid search whose accuracy depends on the chosen grid density. The SFRF methods use approximated trigonometric moments. If the accurate trigonometric moments are available, the SFRF methods coincide with the optimal Bayes solution. Three examples of periodic risks are considered, the MSPE, MAPE, and MCE risks. It is shown that under the MCE risk there exist a tractable estimator. However, under the MSPE and MAPE risks the corresponding estimators cannot be derived analytically for the general case. The SB-SFRF and the FB-SFRF methods can be applied in circular stochastic filtering problems under these risks or any other periodic risk. The superiority of SB-SFRF and FB-SFRF methods w.r.t. state estimation using posterior circular mean is demonstrated in the problem of DOA tracking. A topic for future research is derivation of a method for estimation of a mixed state vector containing both circular and noncircular elements. Another topic is investigating the connection between the considered circular stochastic filtering problems and emerging new approaches, such as sequential deep learning [4], learning of dynamical systems [29], and novel methods for Bayesian filtering with discrete states [41].

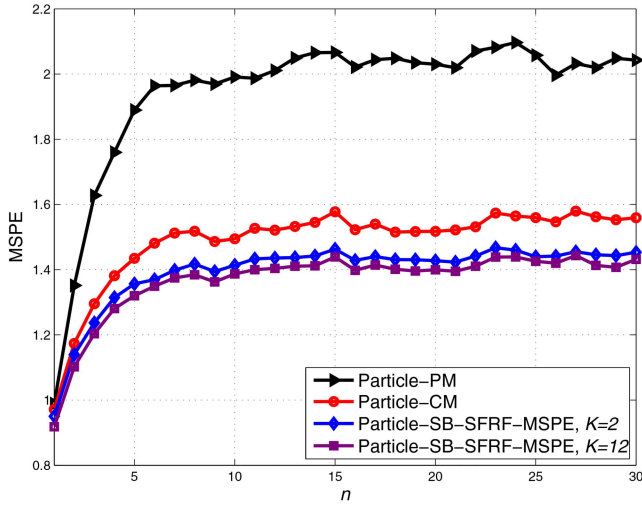


Fig. 14. Unimodal state noise scenario: the MSPEs of Particle-PM, Particle-CM, and Particle-SB-SFRF-MSPE method $K = 2, 12$, with $S = 500$ samples, versus the time step n .

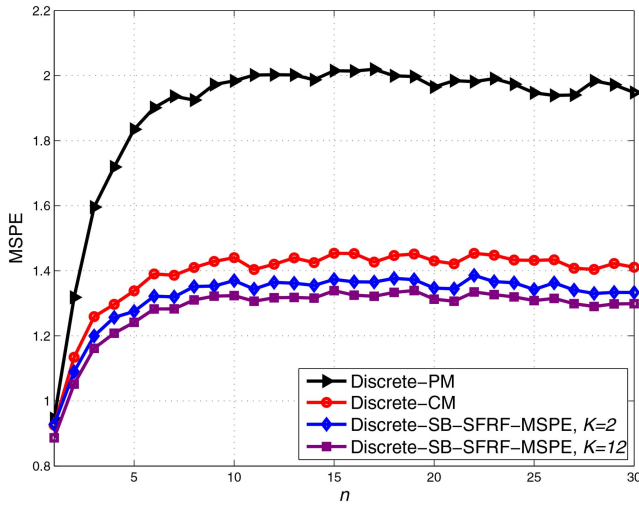


Fig. 15. Unimodal state noise scenario: the MSPEs of Discrete-PM, Discrete-CM, and Discrete-SB-SFRF-MSPE method $K = 2, 12$, with $S = 500$ samples, versus the time step n .

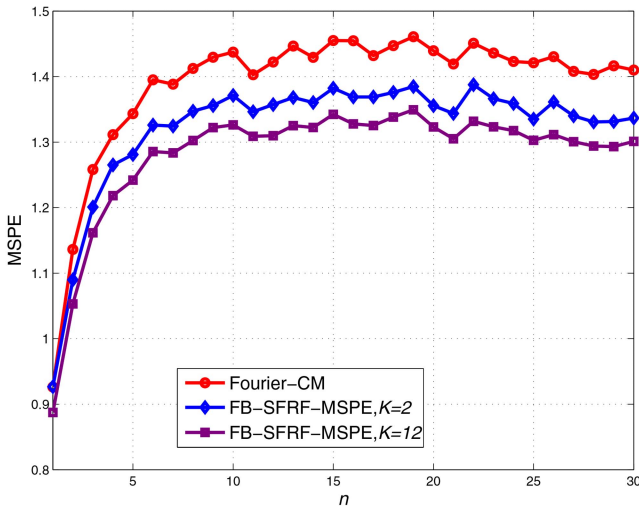


Fig. 16. Unimodal state noise scenario: the MSPEs of Fourier-CM and FB-SFRF-MSPE method $K = 2, 12$, with $D = 40$ Fourier coefficients, versus the time step n .

APPENDIX GENERALIZATION OF THE PREDICTION STAGE UNDER THE APPROACH OF [44] TO AN ARBITRARY STRUCTURE OF $f_{\theta_n|\theta_{n-1}}^{(p)}$

In this appendix, we describe the implementation of the prediction stage, under the approach of [44], with a general $f_{\theta_n|\theta_{n-1}}^{(p)}$, which is not necessarily equal to a function of $\theta_n - \theta_{n-1}$. At each time step n , it is assumed that the function $\sqrt{f_{\theta_n|\theta_{n-1}}^{(p)}}$ can be represented via a two-dimensional Fourier series with Fourier coefficients $\{\phi_{l,m}^{(n,\text{sqr})}\}_{l,m \in \mathbb{Z}}$, i.e.

$$\sqrt{f_{\theta_n|\theta_{n-1}}^{(p)}(\alpha_n | \alpha_{n-1})} = \sum_{l=-\infty}^{\infty} \sum_{m=-\infty}^{\infty} \phi_{l,m}^{(n,\text{sqr})} e^{jl\alpha_n} e^{jm\alpha_{n-1}}. \quad (40)$$

By using (40), it can be verified (see e.g. [8]) that the Fourier coefficients of $f_{\theta_n|\theta_{n-1}}^{(p)} = \sqrt{f_{\theta_n|\theta_{n-1}}^{(p)}} \sqrt{f_{\theta_n|\theta_{n-1}}^{(p)}}$ from (26) are given by the following two-dimensional discrete convolution

$$\phi_{l,m}^{(n)} = \sum_{q=-\infty}^{\infty} \sum_{r=-\infty}^{\infty} \phi_{l-q,r}^{(n,\text{sqr})} \phi_{l,m-r}^{(n,\text{sqr})}, \quad (41)$$

$\forall l, m \in \mathbb{Z}$. In practice, the Fourier coefficients in the r.h.s. of (40) are usually computed numerically and the corresponding two-dimensional Fourier series is truncated. Therefore, the two-dimensional discrete convolution in (41) is finite, resulting in $\tilde{\phi}_{l,m}^{(n)}$ which approximates $\phi_{l,m}$, $\forall l = -D, \dots, D$, $m = -D, \dots, D$. For $|l| > D$ or $|m| > D$, $\phi_{l,m}$ is approximated by zero. The predicted pdf $f_{\theta_n|\mathbf{x}^{(n-1)}}$ is approximated by $f_{n|n-1,\text{FB}}^{(D)} : \Omega_\theta \rightarrow \mathbb{R}$ given by

$$f_{n|n-1,\text{FB}}^{(D)}(y) \triangleq \sum_{l=-D}^D \eta_{l,\text{FB}}^{(n|n-1,D)} e^{ily}, \quad (42)$$

where y is the argument of $f_{n|n-1,\text{FB}}^{(D)}$,

$$\eta_{l,\text{FB}}^{(n|n-1,D)} = 2\pi \sum_{m=-D}^D \eta_{-m,\text{FB}}^{(n-1,D)} \tilde{\phi}_{l,m}^{(n)}, \quad \forall l = -D, \dots, D. \quad (43)$$

Then, the Fourier series representation of $\sqrt{f_{n|n-1,\text{FB}}^{(D)}}$ is derived by applying the procedure, proposed in [44], for obtaining the Fourier coefficients of the square root of a pdf from the Fourier coefficients of the actual pdf.

REFERENCES

- [1] B. D. Anderson and J. B. Moore. Optimal filtering. Englewood Cliffs, NJ: Prentice-Hall, 1979.
- [2] M. S. Arulampalam, S. Maskell, N. Gordon, and T. Clapp. A tutorial on particle filters for online nonlinear/non-Gaussian Bayesian tracking. IEEE Transactions on Signal Processing, 50, 2 (Feb. 2002), 174–188.
- [3] M. Azmani, S. Reboul, J.-B. Choquel, and M. Benjelloun. A recursive fusion filter for angular data. In Proceedings of the IEEE International Conference on Robotics and Biomimetics (ROBIO), Dec. 2009, 882–887.

- [4] M. Baccouche, F. Mamalet, C. Wolf, C. Garcia, and A. Baskurt
Sequential deep learning for human action recognition.
In *Human Behavior Understanding*, 2011, 29–39.
- [5] S. Basu and Y. Bresler
A global lower bound on parameter estimation error with periodic distortion functions
IEEE Transactions on Information Theory, 46, 3 (May 2000), 1145–1150.
- [6] I. Bilik and J. Tabrikian
Maneuvering target tracking in the presence of glint using the nonlinear Gaussian mixture Kalman filter.
IEEE Transactions on Aerospace and Electronic Systems, 46, 1 (Jan. 2010), 246–262.
- [7] D. Brunn, F. Sawo, and U. D. Hanebeck
Efficient nonlinear Bayesian estimation based on Fourier densities.
In *Proceedings of the IEEE International Conference on Multisensor Fusion and Integration for Intelligent Systems*, Sep. 2006, 317–322.
- [8] D. Brunn, F. Sawo, and U. D. Hanebeck
Nonlinear multidimensional Bayesian estimation with Fourier densities.
In *Proceedings of the 45th IEEE Conference on Decision and Control*, Dec. 2006, 1303–1308.
- [9] J. A. Carta, C. Bueno, and P. Ramírez
Statistical modelling of directional wind speeds using mixtures of von Mises distributions: case study.
Energy conversion and management, 49, 5 (2008), 897–907.
- [10] Z. Chen
Bayesian filtering: From Kalman filters to particle filters, and beyond.
Statistics, 182, 1 (2003), 1–69.
- [11] M. Costa, V. Koivunen, and H. V. Poor
Estimating directional statistics Using wavefield modeling and mixtures of von-Mises distributions.
IEEE Signal Processing Letters, 21, 12 (Dec. 2014), 1496–1500.
- [12] G. A. Einicke and L. B. White
Robust extended Kalman filtering.
IEEE Transactions on Signal Processing, 47, 9 (Sep. 1999), 2596–2599.
- [13] N. J. Gordon, D. J. Salmond, and A. F. M. Smith
Novel approach to nonlinear/non-Gaussian Bayesian state estimation.
IEE Proceedings F—Radar and Signal Processing, 140, 2 (Apr. 1993), 107–113.
- [14] S. R. Jammalamadaka and A. Sengupta
Topics in circular statistics.
World Scientific, 2001, vol. 5.
- [15] S. J. Julier and J. K. Uhlmann
Unscented filtering and nonlinear estimation.
Proceedings of the IEEE, 92, 3 (Mar. 2004), 401–422.
- [16] X. Kai, C. Wei, and L. Liu
Robust extended Kalman filtering for nonlinear systems with stochastic uncertainties.
IEEE Transactions on Systems, Man, and Cybernetics—Part A: Systems and Humans, 40, 2 (Mar. 2010), 399–405.
- [17] R. E. Kalman
A new approach to linear filtering and prediction problems.
Journal of Fluids Engineering, 82, 1 (1960), 35–45.
- [18] J. H. Kotecha and P. M. Djuric
Gaussian sum particle filtering.
IEEE Transactions on Signal Processing, 51, 10 (Oct. 2003), 2602–2612.
- [19] R. J. Kozick and B. M. Sadler
Maximum-likelihood array processing in non-Gaussian noise with Gaussian mixtures.
IEEE Transactions on Signal Processing, 48, 12 (Dec. 2000), 3520–3535.
- [20] G. Kurz, I. Gilitschenski, and U. D. Hanebeck
Recursive nonlinear filtering for angular data based on circular distributions.
In *Proceedings of the American Control Conference (ACC)*, June 2013, 5439–5445.
- [21] G. Kurz, I. Gilitschenski, and U. D. Hanebeck
Nonlinear measurement update for estimation of angular systems based on circular distributions.
In *Proceedings of the American Control Conference (ACC)*, June 2014, 5694–5699.
- [22] G. Kurz, I. Gilitschenski, and U. D. Hanebeck
Recursive Bayesian filtering in circular state spaces.
arXiv preprint arXiv:1501.05151 (2015).
- [23] G. Kurz, I. Gilitschenski, S. Julier, and U. D. Hanebeck
Recursive estimation of orientation based on the Bingham distribution.
In *Proceedings of the 16th International Conference on Information Fusion (FUSION)*, July 2013, 1487–1494.
- [24] G. Kurz, I. Gilitschenski, F. Pfaff, and L. Drude
libDirectional, 2015.
Homepage: <https://github.com/libDirectional>.
- [25] E. L. Lehmann and G. Casella
Theory of Point Estimation, 2nd edition.
Springer Texts in Statistics. New York: Springer, 1998.
- [26] J. Leitão and J. Moura
Acquisition in phase demodulation: application to ranging in radar/sonar systems.
IEEE Transactions on Aerospace and Electronic Systems, 31, 2 (Apr. 1995), 581–599.
- [27] J. Q. Li and A. R. Barron
Mixture density estimation.
In *Advances in Neural Information Processing Systems*, 12, (1999).
- [28] X. R. Li and V. P. Jilkov
Survey of maneuvering target tracking. Part V. Multiple-model methods.
IEEE Transactions on Aerospace and Electronic Systems, 41, 4 (Oct. 2005), 1255–1321.
- [29] F. Lindsten
Particle filters and Markov chains for learning of dynamical systems.
Ph.D. dissertation, Linköping University, Linköping, Sweden, 2013.
- [30] J. T.-H. Lo and A. S. Willsky
Estimation for rotational processes with one degree of freedom.
DTIC Document, Technical report, 1972.
- [31] B. C. Lovell and R. C. Williamson
The statistical performance of some instantaneous frequency estimators.
IEEE Transactions on Signal Processing, 40, 7 (July 1992), 1708–1723.
- [32] K. V. Mardia and P. E. Jupp
Directional Statistics.
Wiley Series in Probability and Statistics. Chichester: Wiley, 1999.
- [33] I. Markovic, F. Chaumette, and I. Petrovic
Moving object detection, tracking and following using an omnidirectional camera on a mobile robot.
In *Proceedings of the IEEE International Conference on Robotics and Automation (ICRA)*, May 2014, 5630–5635.

- [34] I. Markovic and I. Petrovic
Bearing-only tracking with a mixture of von Mises distributions.
In Proceedings of the IEEE/RSJ International Conference on Intelligent Robots and Systems (IROS), Oct. 2012, 707–712.
- [35] R. G. McWilliam, B. G. Quinn, and I. V. L. Clarkson
Direction estimation by minimum squared arc length.
IEEE Transactions on Signal Processing, 60, 5 (May 2012), 2115–2124.
- [36] N. Nikolaidis and I. Pitas
Nonlinear processing and analysis of angular signals.
IEEE Transactions on Signal Processing, 46, 12 (Dec. 1998), 3181–3194.
- [37] E. Nitzan, T. Routtenberg, and J. Tabrikian
Cyclic Bayesian Cramér-Rao bound for filtering in circular state space.
In Proceedings of the 18th International Conference on Information Fusion (FUSION), July 2015, 734–741.
- [38] E. Nitzan, T. Routtenberg, and J. Tabrikian
A New Class of Bayesian Cyclic Bounds for Periodic Parameter Estimation.
IEEE Transactions on Signal Processing, 64, 1 (Jan. 2016), 229–243.
- [39] E. Nitzan, T. Routtenberg, and J. Tabrikian
Mean-cyclic-error lower bounds via integral transform of likelihood-ratio function.
Accepted to the 9th IEEE Sensor Array and Multichannel Signal Processing Workshop (SAM), July 2016.
- [40] E. Nitzan, J. Tabrikian, and T. Routtenberg
Bayesian cyclic bounds for periodic parameter estimation.
In Proceedings of the 5th IEEE International Workshop on Computational Advances in Multi-Sensor Adaptive Processing (CAMSAP), Dec. 2013, 308–311.
- [41] M. Nyolt and T. Kirste
On resampling for Bayesian filters in discrete state spaces.
In Proceedings of the IEEE 27th International Conference on Tools with Artificial Intelligence (ICTAI), Nov. 2015, 526–533.
- [42] A. V. Oppenheim and R. W. Schaffer
Discrete Time Signal Processing, 3rd edition.
Prentice-Hall, 2010.
- [43] M. Orton and W. Fitzgerald
A Bayesian approach to tracking multiple targets using sensor arrays and particle filters.
IEEE Transactions on Signal Processing, 50, 2 (Feb. 2002), 216–223.
- [44] F. Pfaff, G. Kurz, and U. D. Hanebeck
Multimodal circular filtering using Fourier series.
In Proceedings of the 18th International Conference on Information Fusion (FUSION), July 2015, 711–718.
- [45] D. Rife and R. Boorstyn
Single tone parameter estimation from discrete-time observations.
IEEE Transactions on Information Theory, 20, 5 (Sep. 1974), 591–598.
- [46] T. Routtenberg and J. Tabrikian
MIMO-AR system identification and blind source separation for GMM-distributed sources.
IEEE Transactions on Signal Processing, 57, 5 (May 2009), 1717–1730.
- [47] T. Routtenberg and J. Tabrikian
Bayesian parameter estimation using periodic cost functions.
IEEE Transactions on Signal Processing, 60, 3 (Mar. 2012), 1229–1240.
- [48] T. Routtenberg and J. Tabrikian
Non-Bayesian periodic Cramér-Rao bound.
IEEE Transactions on Signal Processing, 61, 4 (Feb. 2013), 1019–1032.
- [49] T. Routtenberg and J. Tabrikian
Cyclic Barankin-type bounds for non-Bayesian periodic parameter estimation.
IEEE Transactions on Signal Processing, 62, 13 (July 2014), 3321–3336.
- [50] T. Routtenberg and J. Tabrikian
A fresh look at the cyclic Cramér-Rao bound for periodic parameter estimation.
Accepted to the 19th International Conference on Information Fusion (FUSION), July 2016.
- [51] S. Sarkka
On unscented Kalman filtering for state estimation of continuous-time nonlinear systems.
IEEE Transactions on Automatic Control, 52, 9 (Sep. 2007), 1631–1641.
- [52] H. W. Sorenson and D. L. Alspach
Recursive Bayesian estimation using Gaussian sums.
Automatica, 7, 4 (1971), 465–479.
- [53] G. Stienne, S. Reboul, M. Azmani, J.-B. Choquel, and M. Benjelloun
A multi-sensor circular particle filter applied to the fusion of the GPS-L2C channels.
In Proceedings of the 14th International Conference on Information Fusion (FUSION), July 2011, 1–8.
- [54] T. Tao
An introduction to measure theory.
American Mathematical Society, 2011.
- [55] P. Tichavsky, C. H. Muravchik, and A. Nehorai
Posterior Cramér-Rao bounds for discrete-time nonlinear filtering.
IEEE Transactions on Signal Processing, 46, 5 (May 1998), 1386–1396.
- [56] H. L. Van Trees and K. L. Bell
Bayesian Bounds for Parameter Estimation and Nonlinear Filtering/Tracking.
Wiley-IEEE Press, 2007.
- [57] A. S. Willsky
Fourier series and estimation on the circle with applications to synchronous communication—Part I: Analysis.
IEEE Transactions on Information Theory, 20, 5 (Sep. 1974), 577–583.
- [58] A. S. Willsky and J. T.-H. Lo
Estimation for rotational processes with one degree of freedom—Part II: Discrete-time processes.
IEEE Transactions on Automatic Control, 20, 1 (Feb. 1975), 22–30.
- [59] A. Xenaki, P. Gerstoft, and E. Fernandez-Grande
Sparse DOA estimation with polynomial rooting.
In Proceedings of the 3rd International Workshop on Compressed Sensing Theory and its Applications to Radar, Sonar and Remote Sensing (CoSeRa), June 2015, 104–108.
- [60] D. Zachariah, P. Wirfält, M. Jansson, and S. Chatterjee
Line spectrum estimation with probabilistic priors.
Signal Processing, 93, 11 (2013), 2969–2974.
- [61] A. Zygmund
Trigonometric series, 3rd edition.
Cambridge university press, 2002.



Eyal Nitzan received the B.Sc. (cum laude) and M.Sc. (cum laude) degrees in Electrical and Computer Engineering from the Ben-Gurion University of the Negev, Beer-Sheva, Israel, in 2012 and 2014, respectively. He is currently working toward the Ph.D. degree in the Dept. of Electrical and Computer engineering at Ben-Gurion University of the Negev. His research interests include estimation theory, statistical signal processing, and detection theory. He is the recipient of the Best Student Paper Award (1st prize) in IEEE International Workshop on Computational Advances in Multi-Sensor Adaptive Processing (CAMSAP) 2013. He is the recipient of the Negev scholarship awarded to excellent Ph.D. candidates in 2014.



Tirza Routtenberg received the B.Sc. degree (magna cum laude) in bio-medical engineering from the Technion Israel Institute of Technology, Haifa, Israel in 2005 and the M.Sc. (magna cum laude) and Ph.D. degrees in electrical engineering from the Ben-Gurion University of the Negev, Beer-Sheva, Israel, in 2007 and 2012, respectively. She was a postdoctoral fellow with the School of Electrical and Computer Engineering, Cornell University, in 2012–2014. Since October 2014 she is a faculty member at the Department of Electrical and Computer Engineering at Ben-Gurion University of the Negev, Beer-Sheva, Israel. Her research interests include signal processing in smart grid, statistical signal processing, and estimation and detection theory. She was a recipient of the Best Student Paper Award in International Conference on Acoustics, Speech and Signal Processing (ICASSP) 2011 and in IEEE International Workshop on Computational Advances in Multi-Sensor Adaptive Processing (CAMSAP) 2013 (coauthor). She was awarded the Negev scholarship in 2008, the Lev-Zion scholarship in 2010, and the Marc Rich foundation prize in 2011.



Joseph Tabrikian received the B.Sc., M.Sc., and Ph.D. degrees in Electrical Engineering from the Tel-Aviv University, Tel-Aviv, Israel, in 1986, 1992, and 1997, respectively. During 1996–1998 he was with the Department of Electrical and Computer Engineering, Duke University, Durham, NC as an Assistant Research Professor. He is now with the Department of Electrical and Computer Engineering at Ben-Gurion University of the Negev, Beer-Sheva, Israel. He served as Associate Editor of the IEEE Transactions on Signal Processing during 2001–2004 and 2011–2015 and as Associate Editor of the IEEE Signal Processing Letters during 2012–2015. Since 2015 he has been a Senior Area Editor of the IEEE Signal Processing Letters. He served as a member of the IEEE SAM technical committee during 2010–2015 and was the technical program co-chair of the IEEE SAM 2010 workshop. He is co-author of 5 award-winning papers in different IEEE conferences. His research interests include estimation and detection theory and radar signal processing.